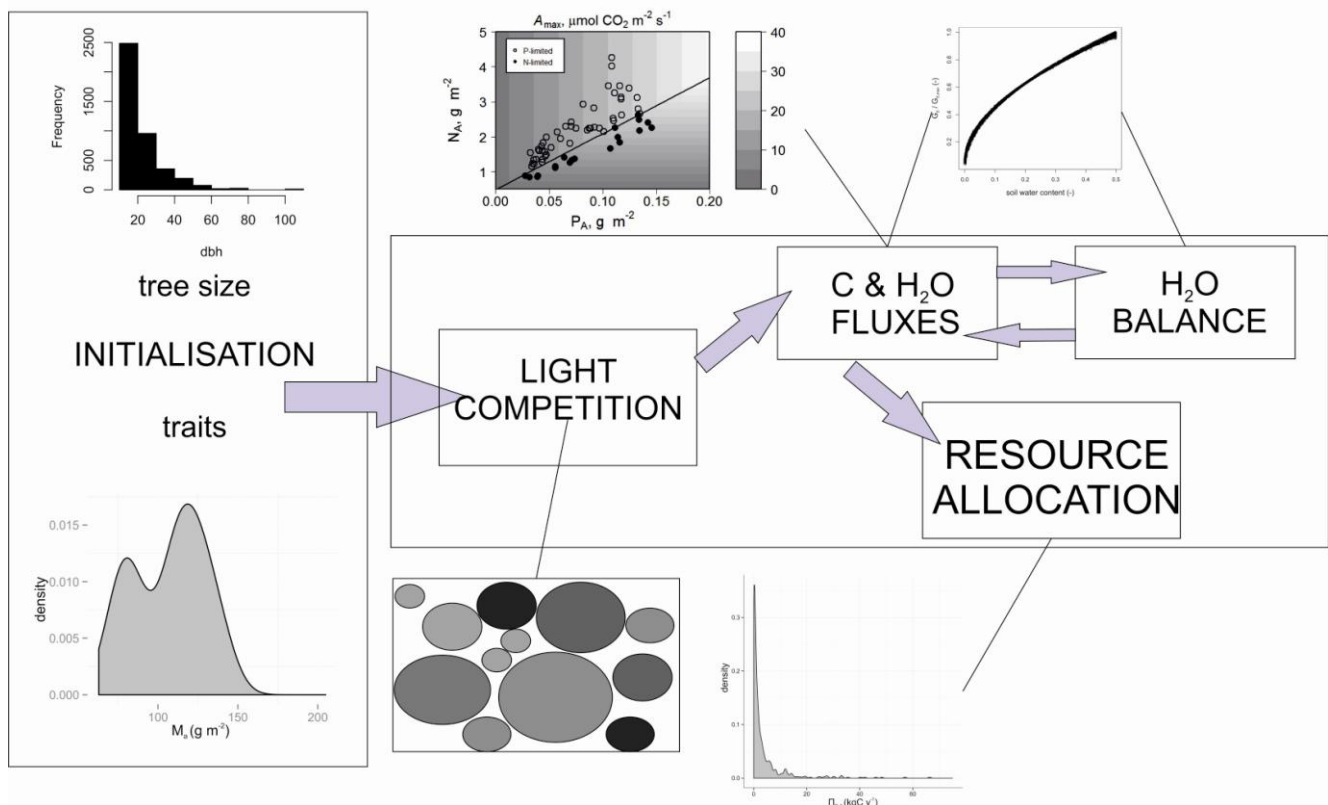


Supplement S1: The Trait-based Forest Simulator (TFS) description

Overview

Trait-based Forest Simulator (TFS) is an individual-based forest model, i.e. it simulates key ecophysiological processes for each tree in a stand. In this version of the model, stand structure is prescribed in terms of the number of trees and distribution of their diameter at breast height (d), although the model is not spatially explicit. The aim of the model is to simulate carbon and water fluxes at small scale forest stands. Here it is parameterised for Amazonian tropical trees although it can be easily adapted to different biomes, given the appropriate data. The model runs on an hourly time-step and it simulates photosynthetic carbon assimilation, growth and maintenance respiration and carbon allocation for each tree in a given stand. Competition for light is approximated through the perfect plasticity model of Purves et al. (2007), assuming flat top canopy trees, i.e. that all of their foliage is found as a disc at the top of their stem. This simple tree architecture approximates light competition, by identifying canopy and sub-canopy trees. Four key functional traits: leaf mass per area [M_a (g m^{-2})], leaf dry mass N and leaf P concentrations [N_{Lm} and P_{Lm} respectively (mg g^{-1})] as well as wood density [D_w (g cm^{-3})] are also predefined for each stand, based on data presented in Baker et al. (2009) and Fyllas et al. (2009). A Monte-Carlo method is used to initialise tree properties, based on the observed stand level trait distribution by assigning randomly trait values for the four functional characteristics following the observed distributions. The basic components of the model are presented in Fig. A1.

Figure S1.1: The basic components of the model and information flow among them. Tree by tree traits and size initialisation is taking place at the beginning of each simulation. Carbon fluxes are estimated hourly while water fluxes, gross and net primary productivity are estimated on a daily basis.

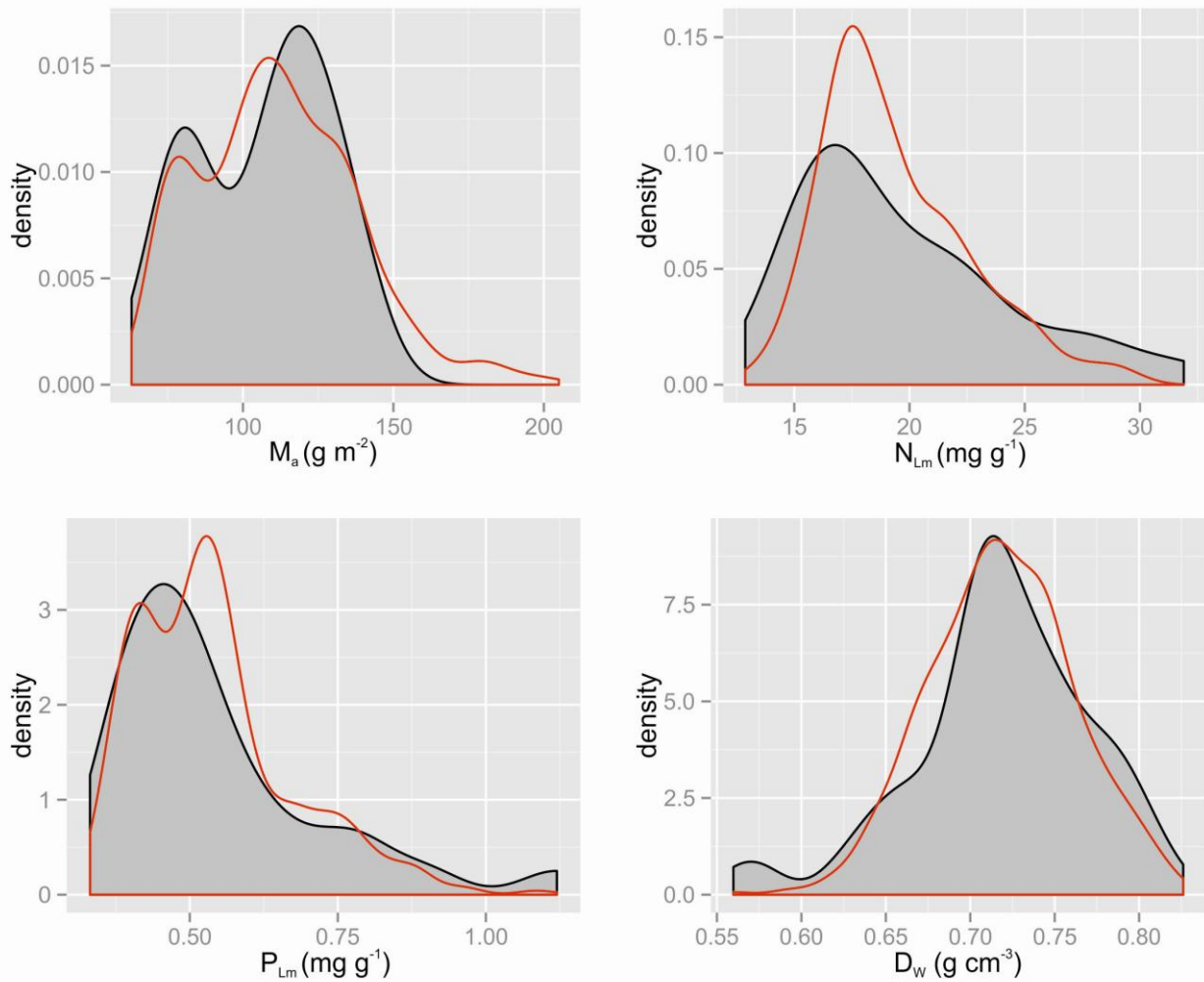


Size and functional traits distributions (Initialisation component)

There is no species or plant functional group description of trees in a TFS stand. The four key functional characters (M_a , N_{Lm} , P_{Lm} and D_w) are used to "define" individuals and capture the importance of functional diversity within a stand. These characters have a direct effect on the architecture and the photosynthetic capacity of a tree. Tree size distribution is prescribed based on the RAINFOR (Malhi et al., 2002) inventory dataset, using d and the four functional traits as the key parameters to estimate other tree components of interest, such as above and below ground biomass, photosynthetic capacity etc.

For the forest stands of interest a set of foliage and structural traits has been recorded and analysed as shown in Patiño et al. (2012) and Fyllas et al. (2009). Thus a sample distribution of M_a , N_{Lm} , P_{Lm} and D_w , is known for each study site. In order to assign the four key traits to each one of trees recorded in the inventory data, a data-driven random vector generation algorithm has been employed (Taylor & Thompson, 1986). The purpose of this algorithm is to generate random trait suites based on the multivariate trait sample of each site by maintaining the underlying distribution. An example of the recorded and generated distributions can be found in Fig. A2.

Figure S1.2: Generation of pseudo-observations of functional traits suites in BNT-04, using the Taylor & Thompson (1986) algorithm embedded in TFS. The observation sample consisted of 28 trait suites, with 620 pseudo-observations generated. Observed distribution of M_a , N_{Lm} , P_{Lm} , and D_w displayed in grey colour, with red colour for the generated ones.



Definition, Allometry and Stoichiometry of Individual Trees in TFS

Each tree is defined as a stem with a flat circular canopy at its top. The four key functional characters (M_a , N_{Lm} , P_{Lm} and D_w) are used to separate between individuals. These characters have a direct effect on a tree's architecture and growth through the regulation of the amount of foliage a tree can support as well as the photosynthetic capacity of leaves.

Tree height [$H(m)$], Crown Area [$C_A(m^2)$] and Crown Depth [$C_D(m)$] are calculated using the allometric equations in Poorter et al. (2006) and are not related with any of the functional traits:

$$H = 61.7 \cdot (1 - \exp(-0.0352 \cdot d^{0.694})) \quad (A1)$$

$$C_A = \exp -1.853 + 1.888 \cdot \log(H) \quad (A2)$$

$$C_D = \exp -1.169 + 1.098 \cdot \log(H) \quad (A3)$$

Total aboveground biomass B_{ABG} (kg) is calculated using equation from Chave (2005), which takes into account the diameter, the height and the D_w of a tree:

$$B_{ABG} = 0.0509 \cdot d^2 \cdot D_w \cdot H \quad (A4)$$

Total root (B_R) and stem (B_S) biomass are estimated from the equations of Niklas (2005) and Enquist & Niklas (2002) respectively:

$$B_R = 0.034 \cdot (B_{ABG})^{0.941} \quad (A5)$$

$$B_S = 2.610 \cdot (B_R)^{1.100} \quad (A6)$$

Foliage area (L_A m²) is given from

$$L_A = L_D \cdot C_V \quad (A7),$$

with C_V the crown volume (m³), estimated as

$$C_V = C_A C_D \quad (A8)$$

and assuming that leaf area density (L_D) decreases with height (Meir et al., 2000) based on the equation:

$$L_D = 0.5 - 0.3 \frac{H}{H_{\max}} \quad (A9), \text{ where } H_{\max} \text{ the height of the tallest tree in the canopy.}$$

The foliage biomass (B_L (kg)) is then:

$$B_L = 0.001 \cdot M_a L_A \quad (A10)$$

With fine root biomass (B_{FR}) assumed to be equal to leaf biomass and thus:

$$B_{FR} = B_L \text{ and } B_{CR} = B_R - B_{FR} \quad (A11) \text{ the coarse root biomass } (B_{CR}).$$

Thus trees with a higher D_w have a higher stem and root biomass, while trees with higher M_a support a higher leaf biomass and thus have a relative higher maintenance cost (through respiration).

The tree level leaf area index (L) is a central variable in terms of estimating the absorbed radiation and scaling the photosynthetic capacity of each tree. Tree specific leaf area index (L) is estimated as:

$$L = \frac{L_A}{C_A} \quad (A12)$$

The nitrogen content of each biomass component is estimated using the scaling relationships of Kerkhoff et al. (2006), when N_L is known. Thus the N concentration in stems (N_S) and roots (N_R) are given from a scaling relationship of the form:

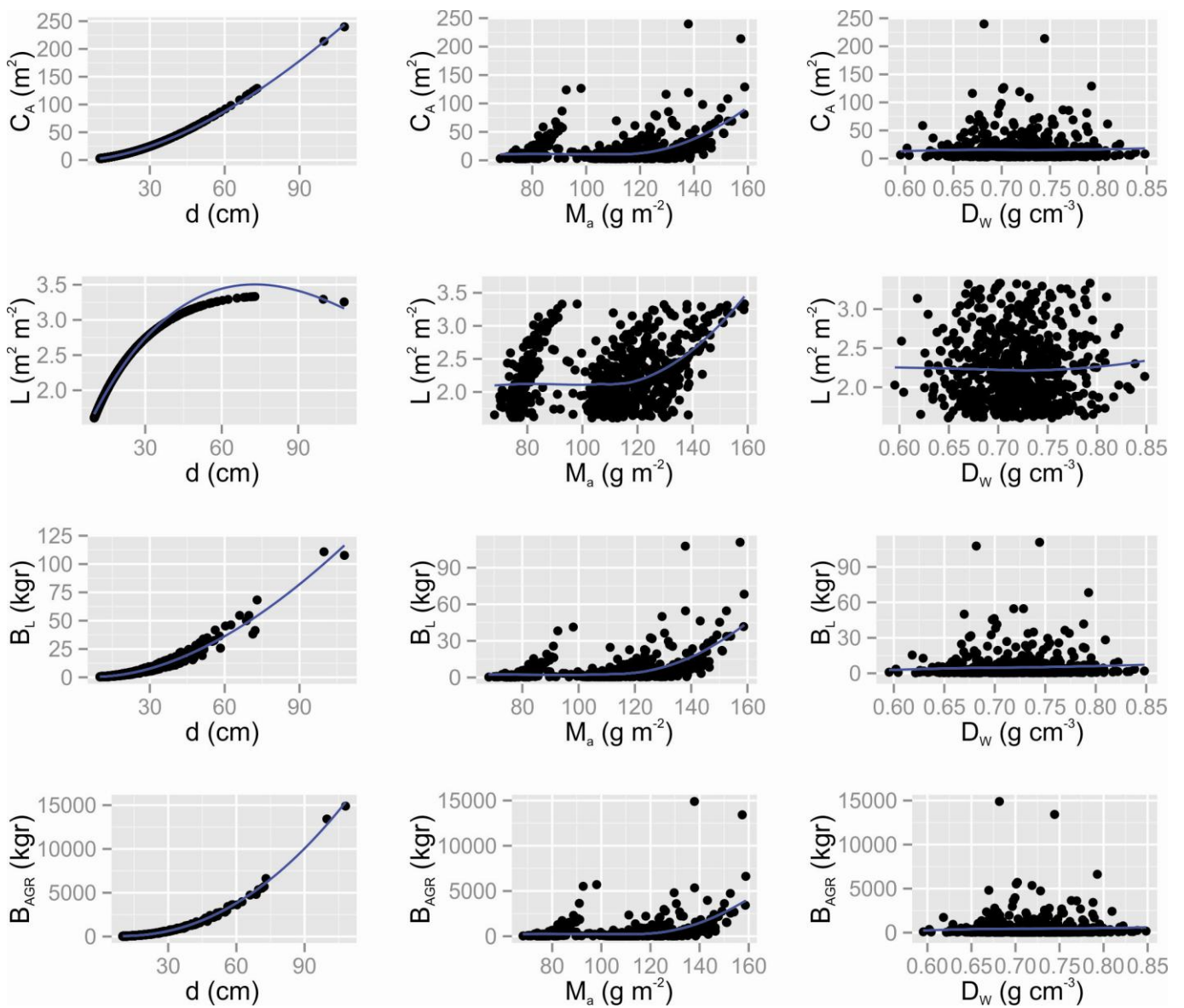
$$N_S = a_S \cdot (N_{Lm})^{b_S} \quad (\text{A13a})$$

$$N_R = a_R \cdot (N_{Lm})^{b_R} \quad (\text{A13b})$$

with a_S , b_S , a_R and b_R empirical coefficients given in Kerkhoff et al. (2006).

The way the basic tree architecture changes with the size of the tree and relates to key functional characters is summarised in Fig. A3.

Figure S1.3: Tree-level C_A , L , B_L and B_{AGR} for each tree in plot BNT-04 against diameter at breast height (d), leaf dry mass per area (M_a) and wood density (D_w)



The leaf-level photosynthetic rates are driven by V_{max} and J_{max} ($\mu\text{mol m}^{-2} \text{s}^{-1}$) which are potentially limited by either the leaf N (N_L) or P (P_L) concentrations (mass basis), according to the formula:

$$V_{\max} = \min(a_{NV} + v_{NV}N_L, a_{PV} + v_{PV}P_L) \times M_a \quad (\text{A14})$$

$$J_{\max} = \min(a_{NJ} + v_{NJ}N_L, a_{PJ} + v_{PJ}P_L) \times M_a \quad (\text{A15})$$

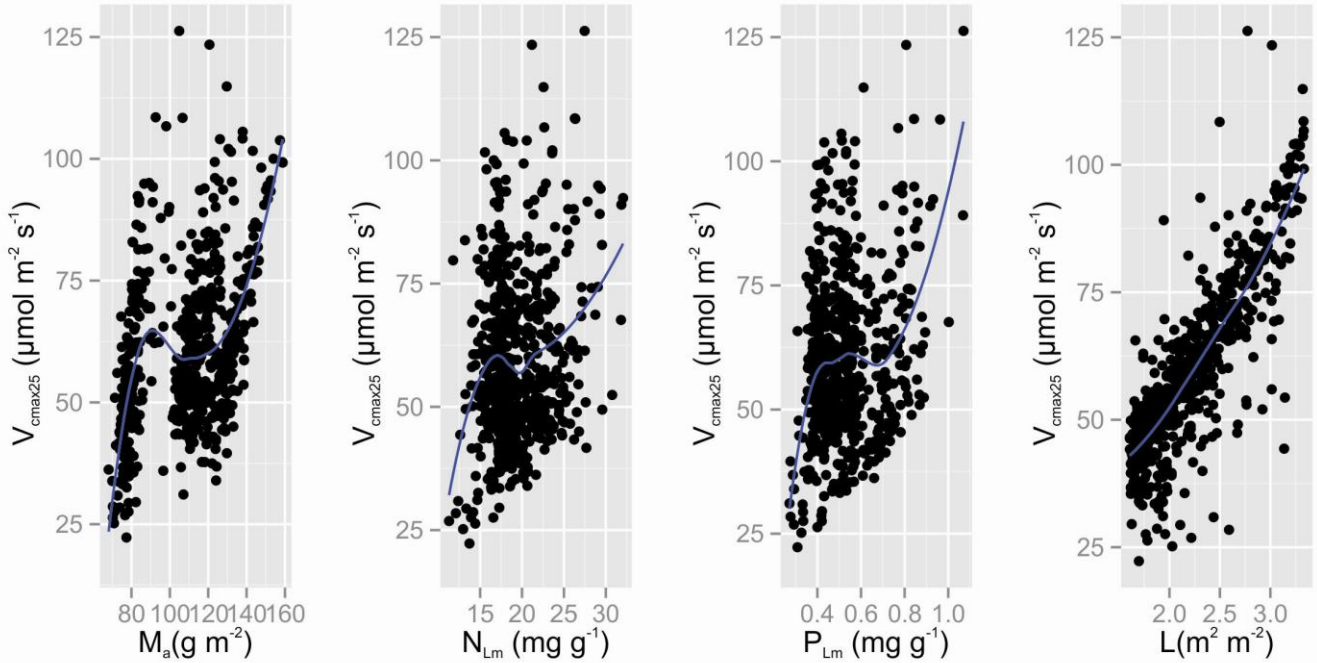
with a_{NV} , a_{NJ} , a_{PV} , a_{PJ} in ($\mu\text{mol g}^{-1} \text{s}^{-1}$) and v_{NV} , v_{NJ} , v_{PV} , v_{PJ} in ($\text{mmol g}^{-1} \text{s}^{-1}$) empirical coefficients (Domingues et al., 2010).

The canopy level photosynthetic capacity (V_{Cmax}) is then estimated by integrating the leaf level V_{max} for the leaf area index of each tree, i.e.:

$$V_{Cmax} = \frac{L \cdot V_{\max} \cdot [1 - \exp(-k_v)]}{k_v} \quad (\text{A16})$$

where $k_v = k_N \cdot L$ and $k_N = \exp(0.00963 V_{\max} - 2.43)$ (17), as suggested in Lloyd et al. (2010). Changes of V_{Cmax} with N_{Lm} , P_{Lm} , M_a and L are summarised in Fig. A4.

Figure S1.4: Canopy level V_{Cmax} for each tree in BNT-04 as a function of N_{Lm} , P_{Lm} , M_a and L



Canopy Architecture and Radiation Environment

The flat-top version of the perfect plasticity model of Purves et al. (2007) has been used in the current version of TFS to characterise canopy and sub-canopy trees (in or out of the canopy). The flat-top version assumes that all of a tree's foliage is found at the top of its stem. A canopy height Z^* is estimated for a forest stand defining canopy and sub-canopy trees. By summing up the crown area (C_A) of all trees in the stand, Z^* is defined as the height of the last tree that enters the sum before the cumulative crown area is equal to the plot area.

Canopy trees are absorbing a mean daily amount of shortwave solar radiation equal to the sum of mean beam, diffuse and scattered daily radiation (all in Wm^{-2}), i.e. $S_{can} = S_{beam} + S_{diffuse} + S_{scattered}$ while sub-canopy tree only receive $S_{sub} = S_{diffuse} + S_{scattered}$, in correspondence to the sun-shade model of de Pury and Farquhar (1997). Thus based on Wang & Leuning (1998):

$$S_{\text{can}} = Q_d(1 - \rho_d)k_d^* \Psi \langle k_d^* + k_b \rangle + Q_b(1 - \rho_b)k_b^* \Psi \langle k_b^* + k_b \rangle + Q_b(1 - \omega)k_b [\Psi \langle k_b \rangle - \Psi \langle 2k_b \rangle] \quad (18a)$$

$$S_{\text{sub}} = Q_d(1 - \rho_d)k_d^* [\Psi \langle k_d^* \rangle - \Psi \langle k_d^* + k_b \rangle] + Q_b(1 - \rho_b)k_b^* [\Psi \langle k_b^* \rangle - \Psi \langle k_b^* + k_b \rangle] - Q_b(1 - \omega)k_b [\Psi \langle k_b \rangle - \Psi \langle 2k_b \rangle] \quad (18b)$$

$$\text{with } \Psi \langle x \rangle = \frac{1 - \exp(-x \cdot L)}{x} \quad (18c)$$

where Q_b and Q_d are hourly mean shortwave direct and diffuse radiation (both in Wm^{-2}); ρ_b , ρ_d and ω are leaf direct beam reflectance, leaf diffuse reflectance and leaf scattering coefficient, all unitless; k_b , k_b^* , k_d , k_d^* are black leaves beam, black leaves diffuse, canopy beam and canopy diffuse extinction coefficients. Estimation of the direct and diffuse fraction of solar radiation is achieved by implementing the Spitters et al. (1986) approximation.

The longwave radiation absorbed by canopy trees and sub-canopy trees (both in Wm^{-2}) is given by:

$$L_{\text{can}} = -k_d \sigma T_a^2 \varepsilon_l (1 - \varepsilon_a) \Psi \langle k_b + k_d \rangle + (1 - \varepsilon_s)(\varepsilon_l - \varepsilon_a) \Psi \langle 2k_d \rangle \Psi \langle k_b - k_d \rangle \quad (19a)$$

and

$$L_{\text{sub}} = -k_d \sigma T_a^2 \varepsilon_l (1 - \varepsilon_a) \Psi \langle k_b \rangle - (1 - \varepsilon_s) \varepsilon_l - \varepsilon_a \exp(-k_d \cdot L) \Psi \langle k_d \rangle - L_{\text{can}} \quad (20)$$

respectively. This is as suggested in Wang & Leuning (1998). Here ε_l , ε_a and ε_s are the leaf, sky and soil emissivity, with ε_a being estimated by the formula of Brutsaert (1975).

Photosynthesis

The Farquhar et al. (1980) model of leaf photosynthesis is used to estimate mean hourly rates of carbon assimilation at the leaf level. As discussed above the maximum photosynthetic rate is regulated by N_L or P_L through the co-limitation model of Domingues et al. (2010). The Rubisco limited net assimilation rate ($\mu\text{mol m}^{-2} \text{s}^{-1}$) is given by the equation:

$$A_v^* = V_{C_{\text{max}}} \left(\frac{C_c - \Gamma^*}{K_C \left(1 + \frac{p_{O_2}}{K_O}\right) + C_c} \right) \quad (A21)$$

where C_c is the CO_2 concentration in the chloroplast ($\mu\text{mol mol}^{-1}$), Γ^* the CO_2 compensation point, p_{O_2} the intercellular partial pressure of O_2 , K_C and K_O are the Michaelis-Menton constants for carboxylation and oxygenation by Rubisco. A_v^* is the assimilation rate in the absence of leaf respiration in the light, which is estimated later on. The light limited assimilation rate ($\mu\text{mol m}^{-2} \text{s}^{-1}$) is estimated according to:

$$A_J = \frac{J}{4} \left(\frac{C_c - \Gamma^*}{C_c + 2\Gamma^*} \right) \quad (A22)$$

with J the potential rate of electron transport modelled as a non-rectangular hyperbolic function of the absorbed quantum flux (I_2 in $\mu\text{mol quanta m}^{-2} \text{s}^{-1}$), the absorbed irradiance reaching photosystem II (J_{max} in $\mu\text{mol m}^{-2} \text{s}^{-1}$) and the curvature factor θ :

$$\theta J^2 - (I_2 + J_{\text{max}})J + I_2 J_{\text{max}} = 0 \quad (A23)$$

I_2 is estimated from estimates of the amount incoming photosynthetic active radiation (I_0) reaching the foliage of each tree, canopy reflectance (r), transmittance (t) and quantum yield (a) according to

$$I_2 = \alpha_{12} S \quad (\text{A24})$$

with $\alpha_{12}=0.30$ the light use efficiency. Shortwave radiation (either S_{can} or S_{sub}) (Wm^{-2}) is transformed to *PAR* ($\mu\text{mol m}^{-2}\text{s}^{-1}$) by multiplying with a factor of 2.025. The mean hourly net CO_2 assimilation rate (A) is then estimated as the minimum between A_V and A_J . Temperature sensitivities for V_{max} , J_{max} , Γ^* and the CO_2 and O_2 Michaelis constants K_C and K_O respectively, are estimated according to Bernacchi et al. (2001) and Lloyd et al. (1995). Finally, the total daily photosynthetic carbon assimilation for each tree (A_d) is calculated as the sum of hourly A multiplied by the crown area of the tree.

Stomatal Conductance

Maximum (no water stress) stomatal conductance (g_{max}) is estimated following the Medlyn et al. (2011,2012) equation:

$$g_{s,\text{max}} = g_0 + 1.6 \left(1 + \frac{g_1}{\sqrt{D_C}} \right) \frac{A_n}{C_a} \quad (\text{A25})$$

with g_0 ($\text{mol m}^{-2} \text{s}^{-1}$) the minimum stomatal conductance, $g_1(-)$ an empirical coefficient that represents the water use efficiency of the plant, and D_C the leaf-to-atmosphere vapour pressure difference. Values of g_0 and g_1 that lead to the best model performance were different between sites, as indicated by the model calibration procedure. For the basin wide simulations constant values of $g_0=0.020$ ($\text{mol m}^{-2} \text{s}^{-1}$) and $g_1=5.0$ (-) were used, close to the estimates of Domingues et al. (2013). In future versions of the model, g_0 and g_1 should be related with other functional traits. The optimum stomatal conductance is subsequently reduced to the actual g_s by multiplying the second term of equation A25 with the water stress coefficient described in the “Water Balance and Soil Water Stress” section.

Respiration

Tree respiration includes a growth and a maintenance component, computed daily. Growth respiration is considered as a constant fraction of daily photosynthesis equal to 0.25 (Cannell & Thornley, 2000). In TFS three alternative formulations to calculate maintenance respiration are implemented.

Mori Method

The first method to estimate the maintenance respiration of a tree is based on the Mori et al. (2010) empirical model. In this model a mixed-power scaling equation is being used which only takes into account the size of a tree to estimate the total maintenance respiration R_m ($\mu\text{mol CO}_2 \text{s}^{-1}$):

$$R_m = -\log \left[\frac{1}{GB_{\text{tot}}^g} + \frac{1}{HB_{\text{tot}}^h} \right] \quad (\text{A26})$$

with $B_{\text{tot}}=B_{\text{ABG}}+B_{\text{R}}$ the total tree biomass and g , h , G and H empirical coefficients provided in Mori et al. (2010) viz $g=1.408$, $h=0.805$, $G=201.87$ and $H=0.410$.

Modified Reich Method

The second method is based on findings of a strong coupling between respiration rates and nitrogen content of different plant components (Reich et al., 2008). Maintenance respiration rates of leaves, stems and roots are calculated based on their mass and nitrogen content. The nitrogen content of each component is estimated using the scaling relationships of Kerkhoff et al. (2006), when N_L is known (equations A13a and A13b).

Stem (R_{mS}) and coarse root (R_{mCR}) respiration rates are expressed as a function of their nitrogen content. Leaf maintenance respiration R_{mL} is not estimated as in Reich et al. (2008), but it is rather coupled to photosynthesis assuming it represents a constant fraction of V_{max} (Scheiter & Higgins, 2009), in order to account for potential N and/or P limitations. Fine root respiration R_{mFR} is assumed to be equal to R_{mL} . After transforming N_S and N_R in (mmol g^{-1}) the maintenance respiration of each component is given as:

$$R_{mL} = 0.015 V_{Cmax} \quad (\text{A27}) \quad \text{in } \mu\text{mol CO}_2 \text{ s}^{-1}$$

$$R_{mS} = g(T) \alpha_{SS} B_S \tau_S N_S^{\sigma_S} \quad (\text{A28}) \quad \text{in } \text{nmol CO}_2 \text{ s}^{-1}$$

$$R_{mCR} = g(T) \alpha_{RS} B_{CR} \tau_R N_R^{\sigma_R} \quad (\text{A29}) \quad \text{in } \text{nmol CO}_2 \text{ s}^{-1}$$

with τ_i and σ_i empirical coefficients reported in Reich et al. 2008 and $g(T)$ the temperature dependence function of Tjoelker et al. (2001). Here α_{SS} and α_{RS} are the sapwood fractions of stem and coarse root biomass (both considered constant with size) and equal to 0.025 (Scheiter & Higgins, 2009). Thus the overall maintenance respiration (R_m in kg C) is given from equation:

$$R_m = R_{mL} + R_{mS} + R_{mFR} + R_{mCR} \quad (\text{A30})$$

Sapwood Volume Method

The third method is a combined approach which replaces the use of a constant sapwood fraction for stems. Total maintenance respiration is again divided to leaf, stem and root respiration (equation 30). Foliage respiration is again estimated as a fraction of V_{max} (equation A27) and fine root respiration is assumed to be equal to foliage respiration. Stem maintenance respiration is calculated as:

$$R_{mS} = g(T) \delta S_V \quad (\text{A31})$$

with S_V the sapwood volume and δ ($39.6 \mu\text{mol CO}_2 \text{ s}^{-1} \text{ m}^{-3}$) a respiration rate per sapwood volume measured for tropical trees (Ryan et al., 1994). Sapwood volume is estimated by inverting the pipe model and assuming that the ratio of leaf area to sapwood area (Φ_{LS}) increases with the height and the wood density for tropical trees following (Calvo-Alvarado et al., 2008; Meinzer et al., 2008):

$$\Phi_{LS} = 0.5 \times (\lambda_1 + \lambda_2 \cdot H + \delta_1 + \delta_2 D_w) \quad (\text{A32}),$$

with $\lambda_1 = 0.066 \text{ m}^2 \text{ cm}^{-2}$, $\lambda_2 = 0.017 \text{ m cm}^{-2}$, $\delta_1 = -0.18 \text{ m}^2 \text{ cm}^{-2}$ and $\delta_2 = 1.6 \text{ cm}^3 \text{ g}^{-1}$. Sapwood area (m^2) and volume (m^3) are then calculated from:

$$S_A = L_A / \Phi_{LS} \quad (\text{A33}) \quad \text{and}$$

$$S_V = S_A \cdot (H - C_D) \quad (\text{A34})$$

Coarse root maintenance respiration is estimated as in (Scheiter & Higgins, 2009):

$$R_{mCR} = 0.218 \cdot \frac{\alpha_{RS} \cdot B_{CR}}{\Phi_{CN}} \cdot g(T) \quad (\text{A35}) \quad \text{where } \Phi_{CN} \text{ is the root C:N ratio estimated on the basis of the simulated } N_R$$

assuming a dry weight carbon fraction of 0.5.

Water Balance and Soil Water Stress

A single-layer soil bucket model is used in the current version of the model to estimate soil water content and the down-regulation of stomatal opening in case of limited soil water. We are aware that this is a component that needs further improvement in the future but for the purpose of this study which is to explore to first order the basic functioning of forest stand carbon uptake and water loss a single-layer soil model should be sufficient. In contrast to most ecosystem fluxes model, where photosynthetic rates are directly regulated by water availability (Cox et al. 1998; Clark et al. 2011), we couple water ‘stress’ to reduction of canopy conductance by estimating a daily fractional available soil water content \mathcal{G}_i , for each i tree in the stand given from:

$$\mathcal{G}_i = \left[\frac{W_i - W_w}{W_{FC} - W_w} \right] \quad (\text{A36}),$$

where W_i the available water for tree i , W_{FC} is the soil water content at field capacity (matric potential of 0.033 MPa) and W_w is the soil water content at wilting (matric potential of 1.5MPa), both estimated using the van Genuchten (1980) model with the soil-type specific parameters reported in Hodnett & Tomasella (2002).

The estimation of W_i at time t is summarized in the following graphic and calculated as:

$$W_{i,t} = W_{t-1} + (P_t - E_{\text{tot},t} - Q_t) + Z_{R,i} - Z_D \quad (\text{A37})$$

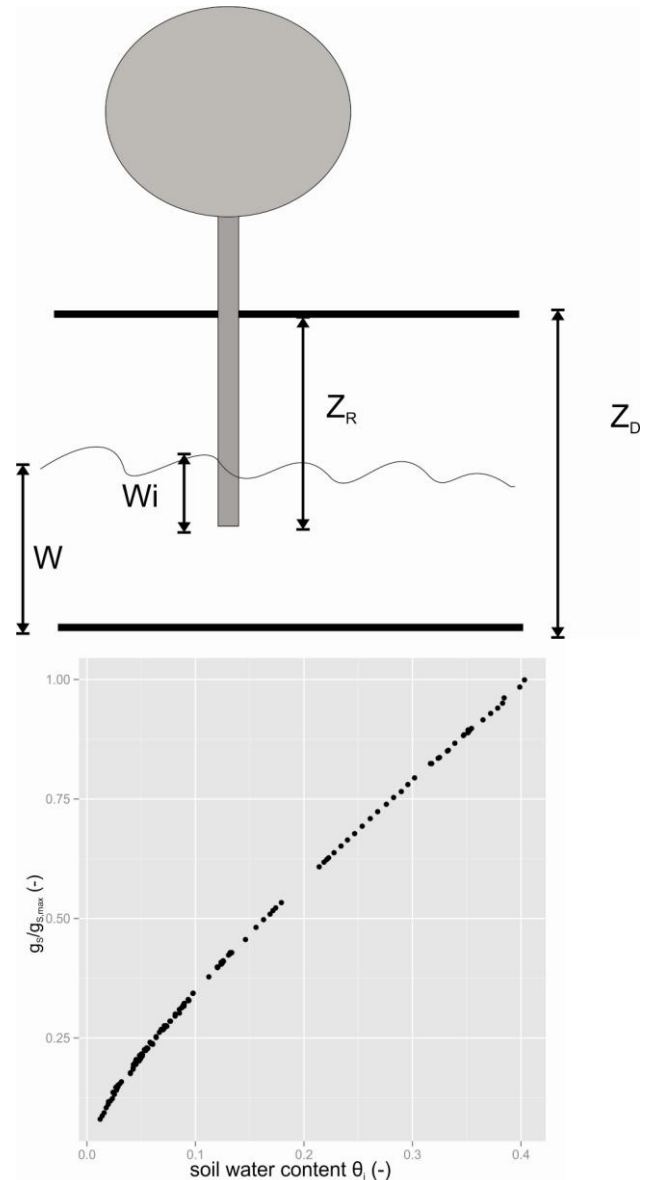
Here W_{t-1} is the previous day's (stand level) soil water column, P_t is the daily total precipitation, $E_{\text{tot},t}$ the daily total (stand level) evaporation, Q_t the run-off, $Z_{R,i}$ is the root depth of tree i , and Z_D the soil depth all expressed in mm. The rooting depth of each tree is estimated in a similar way to Scheiter and Higgins (2009), as the biomass needed to construct a root cylinder of radius R_r ($R_r = 0.15\text{m}$) with a density D_r ($D_r = 100 \text{ kg m}^{-3}$):

$$Z_R = \frac{B_{FR}}{\pi D_r R_r^2} \quad (\text{A38})$$

A tree specific water stress term γ_i that has a direct effect on stomatal conductance (as a multiplier) is subsequently estimated from, $\gamma_i = \mathcal{G}_i^n$ (A 39)

As discussed in Keenan et al. (2010) the exponent in the last equation, is a measure of the non-linearity of the effects of soil water stress on stomatal conductance. The smaller the value of n , the less sensitive is the overall canopy conductance to soil water stress. In our case we found a value of $n=0.5$ to give best agreement with observations in regards to the response of stomatal conductance to changes in water availability and the long-term simulation of carbon fluxes. The way stomatal conductance (given here as the ratio of $g_s/g_{s,max}$) varies with θ_i is graphically illustrated in the following figure.

Figure S1.5: Variation of the $g_s/g_{s,max}$ with soil water content at Caxiuana.



Canopy Transpiration

An iterative procedure (Medlyn et al., 2007) is used to solve the energy balance for the canopy of each tree. The algorithm initially assumes a canopy-to-air vapour pressure deficit D_C equal to the estimated vapour pressure deficit (*i.e.* with leaf temperature (T_L) equal to air temperature) and a chloroplast CO_2 concentration (C_c) of $0.7C_a$. It then calculates leaf photosynthetic rate (A_n) and stomatal conductance (g_s), as well as boundary layer and radiation conductance. Subsequently the Penman-Montheith equation is used to estimate canopy transpiration and then new T_L, D_C and C_c . Convergence is achieved if T_L difference between steps is less than 0.1 degrees °C.

Following Medlyn et al. (2007), the total leaf conductance to heat (g_H) is equal to:

$$g_H = 2 \times (g_{bHf} + g_{bHu} + g_r) \quad (\text{A40})$$

with g_{bHf} the boundary layer conductance for free convection ($\text{mol m}^{-2} \text{s}^{-1}$):

$$g_{bHf} = \frac{0.5D_H(1.6 \cdot 10^8 |T_L - T_a| w^3)^{0.25}}{w} \left(\frac{rP}{RT_K} \right) \quad (\text{A41})$$

$D_H = 21.5 \times 10^{-6} (\text{m}^2 \text{s}^{-1})$ the molecular diffusivity for heat in air, $w = 0.15 (\text{m})$ the leaf width, $R = 8.314 (\text{J mol}^{-1} \text{K}^{-1})$ the universal gas constant and T_K is the leaf temperature in Kelvin.

Similarly g_{bHu} the boundary layer conductance for forced convection ($\text{mol m}^{-2} \text{s}^{-1}$):

$$g_{bHu} = 0.003 \sqrt{\frac{U}{w}} \left(\frac{rP}{RT_K} \right) \quad (\text{A42})$$

U being the wind speed (m s^{-1}) and g_r the radiative conductance ($\text{mol m}^{-2} \text{s}^{-1}$):

$$g_r = 4\varepsilon_l \sigma (T_a + 273.15)^4 k_d e^{-k_d SL} + e^{-k_d(L-L^+)} \quad (\text{A43})$$

with σ the Stefan-Boltzmann constant, L the tree level leaf area index and L^+ the cumulative leaf area shading above a sub-canopy tree (for canopy trees $L^+ = 0$).

The boundary layer conductance to water vapour is estimated by: $g_{bV} = 1.075 (g_{bHf} + g_{bHu}) / 0.5$ (A44)

Ultimately the latent heat flux per unit leaf area ($\lambda E \text{ W m}^{-2}$) is given according to the Penman-Monteith equation:

$$\lambda E = \frac{sR_n + g_H c_p \rho_a D_C}{s + \gamma g_H / g_V} \quad (\text{A45})$$

where λ the latent heat of evaporation, R_n the net isothermal radiation (W m^{-2}), c_p the heat capacity of the air ($\text{J kg}^{-1} \text{K}^{-1}$), ρ_a the air density (kg m^{-3}), s the slope of the saturation vapour pressure to temperature curve (Pa K^{-1}), γ the psychrometric constant (Pa K^{-1}) and g_H, g_V expressed in (m s^{-1}).

Table of Symbols

Tree Architecture and Functional Configuration		
Symbol	Variable	Unit, Value
d	Tree Diameter at breast height	cm
H	Tree Height	m
C_A	Tree Crown Area	m ²
C_{Amax}	Maximum Crown Area	m ²
C_D	Crown Depth	m
C_V	Crown Volume	m ³
L_D	Tree foliage density	m ² m ⁻³
L_A	Tree foliage area	m ²
L	Tree Leaf Area Index	m ² m ⁻²
M_a	Leaf dry mass per area	g m ⁻²
N_{Lm}	Leaf dry mass nitrogen content	mg g ⁻¹
N_s	Stem dry mass nitrogen content	mg g ⁻¹
N_R	Root dry mass nitrogen content	mg g ⁻¹
P_{Lm}	Leaf dry mass phosphorus content	mg g ⁻¹
D_W	Wood density of the stem	g cm ⁻³
α_S, β_S	Scaling coefficients for stem N content	(-)
α_R, β_R	Scaling coefficients for root N content	(-)
B_{ABG}	Tree above ground biomass	kg
B_L	Tree Total Leaf biomass	kg
B_S	Tree Stem biomass	kg
B_R	Tree Total root biomass	kg
B_{CR}	Tree Coarse root biomass	Kg
B_{FR}	Tree Fine root biomass	kg
Z_R	Tree Root Depth	mm
Radiation Balance Submodel		
Symbol	Variable	Unit, Value
Z^*	Canopy height from the perfect plasticity model	m
k_b	Direct beam radiation extinction coefficient (black leaves)	0.50 (-)
k_b^*	Direct beam radiation extinction coefficient	0.46 (-)
k_d	Diffuse radiation extinction coefficient (black leaves)	0.78 (-)
k_d^*	Diffuse radiation extinction coefficient	0.719 (-)
ρ_b	Direct beam radiation reflection coefficient	(-)
ρ_d	Diffuse radiation reflection coefficient	0.036
ω	Scattering coefficient of the leaves	0.150
ϵ_l	Emissivity of the leaf	0.96
ϵ_a	Emissivity of the air	(-)
ϵ_s	Emissivity of the soil	0.94 (-)
Q_b	Incoming direct beam radiation	W m ⁻²
Q_d	Incoming diffuse radiation	W m ⁻²
S_{can}	Absorbed shortwave radiation from a canopy tree	W m ⁻²
S_{sub}	Absorbed shortwave radiation from a subcanopy tree	W m ⁻²
L_{sun}	Absorbed longwave radiation from a canopy tree	W m ⁻²
L_{shade}	Absorbed longwave radiation from a subcanopy tree	W m ⁻²

Photosynthesis & Respiration Submodels		
Symbol	Variable	Unit, Value
C_c	CO ₂ concentration in the chloroplast	$\mu\text{mol mol}^{-1}$
C_a	Atmospheric CO ₂ concentration	$\mu\text{mol mol}^{-1}$
T_L	Leaf temperature	$^{\circ}\text{C}$
I_0	PAR reaching the top of the tree canopy	$\mu\text{mol quanta m}^{-2}\text{s}^{-1}$
I_2	Absorbed irradiance by photosystem II	$\mu\text{mol quanta m}^{-2}\text{s}^{-1}$
ϑ	Curvature factor	0.7 (-)
D_c	Vapour pressure deficit between the canopy and the air	mol mol^{-1}
VPD	Vapour pressure deficit of the air	Pa
$g_s, g_{s,\text{max}}$	Stomatal and maximum stomatal conductance	$\text{mol m}^{-2}\text{s}^{-1}$
J, J_{max}	Electron transport rate and maximum electron transport rate	$\mu\text{mol m}^{-2}\text{s}^{-1}$
$V_{\text{cmax}}, V_{\text{Cmax}}$	Leaf and Canopy maximum carboxylation rates	$\mu\text{mol m}^{-2}\text{s}^{-1}$
a_{NV}	Empirical coefficient from the Domingues et al. 2010 model	-1.16 ($\mu\text{mol m}^{-2}\text{s}^{-1}$)
v_{NV}	Empirical coefficient from the Domingues et al. 2010 model	0.70 ($\mu\text{mol mg}^{-1}\text{s}^{-1}$)
a_{PV}	Empirical coefficient from the Domingues et al. 2010 model	-0.30 ($\mu\text{mol m}^{-2}\text{s}^{-1}$)
v_{PV}	Empirical coefficient from the Domingues et al. 2010 model	0.85 ($\mu\text{mol mg}^{-1}\text{s}^{-1}$)
a_{NJ}	Empirical coefficient from the Domingues et al. 2010 model	-1.22 ($\mu\text{mol m}^{-2}\text{s}^{-1}$)
v_{NJ}	Empirical coefficient from the Domingues et al. 2010 model	0.92 ($\mu\text{mol mg}^{-1}\text{s}^{-1}$)
a_{PJ}	Empirical coefficient from the Domingues et al. 2010 model	-0.11 ($\mu\text{mol m}^{-2}\text{s}^{-1}$)
v_{PJ}	Empirical coefficient from the Domingues et al. 2010 model	0.66 ($\mu\text{mol mg}^{-1}\text{s}^{-1}$)
k_V	Empirical coefficient from the Lloyd et al. 2009 model	(-)
k_N	Empirical coefficient from the Lloyd et al. 2009 model	(-)
Γ^*	CO ₂ compensation point	$\mu\text{mol mol}^{-1}$
K_C	Michaelis-Menton carboxylation constant	$\mu\text{mol mol}^{-1}$
K_O	Michaelis-Menton oxygenation constant	mmol mol^{-1}
g_0, g_1	Empirical coefficients in Medlyn et al. 2011 conductance model	$\text{mol m}^{-2}\text{s}^{-1}, (-)$
g_H	Total leaf conductance to heat	$\text{mol m}^{-2}\text{s}^{-1}$
g_{bHf}	Boundary layer conductance for free convection	$\text{mol m}^{-2}\text{s}^{-1}$
g_{bHu}	Boundary layer conductance for forced convection	$\text{mol m}^{-2}\text{s}^{-1}$
g_r	Radiative conductance	$\text{mol m}^{-2}\text{s}^{-1}$
A_n	Rate of net photosynthetic carbon assimilation	$\mu\text{mol m}^{-2}\text{s}^{-1}$
A_v	Rubisco limited photosynthetic rate	$\mu\text{mol m}^{-2}\text{s}^{-1}$
A_j	Electron transfer limited photosynthetic rate	$\mu\text{mol m}^{-2}\text{s}^{-1}$
A_{day}	Daily total photosynthetic carbon assimilation	kgC d^{-1}
R_m	Total tree maintenance respiration	kgC d^{-1}
R_{mL}	Foliage maintenance respiration	$\mu\text{mol m}^{-2}\text{s}^{-1}$
R_{mS}	Stem maintenance respiration	$\mu\text{mol m}^{-2}\text{s}^{-1}$
R_{mCR}	Coarse root maintenance respiration	$\mu\text{mol m}^{-2}\text{s}^{-1}$
R_{mFR}	Fine root maintenance respiration	$\mu\text{mol m}^{-2}\text{s}^{-1}$
G, H	Empirical coefficients for the Mori respiration model	
$a_{\text{SS}}, a_{\text{RS}}$	Sapwood fraction of stem and root biomass	0.025
τ_S, σ_S	Empirical coefficients for the Reich stem respiration model	
τ_R, σ_R	Empirical coefficients for the Reich root respiration model	

Climate & Water Balance Submodels		
Symbol	Variable	Unit, Value
P_r	Atmospheric pressure	Pa
T_m	Mean daily air temperature	°C
P	Total daily precipitation	mm
Q	Run Off	mm
E_{tot}	Total Stand Transpiration	mm
ϑ_i	Daily water content available to tree i	mm
ϑ_w	Water content at wilting point	mm
ϑ_{FC}	Water content at field capacity	mm
γ	Water stress term	(-)
Z_s	Soil Depth	mm

Supplement S2: Additional TFS simulations and figures

Figure S2.1: Observed (grey) against simulated (red) histograms of annual NPP allocated to stem growth at each one of the 7 intensive measurements plots. Plots are classified to a fertile and an infertile group based on the site score of the first PCA axis (Fyllas et al., 2009), with upper panel illustrating high fertility plots and lower panel illustrating low fertility plots.

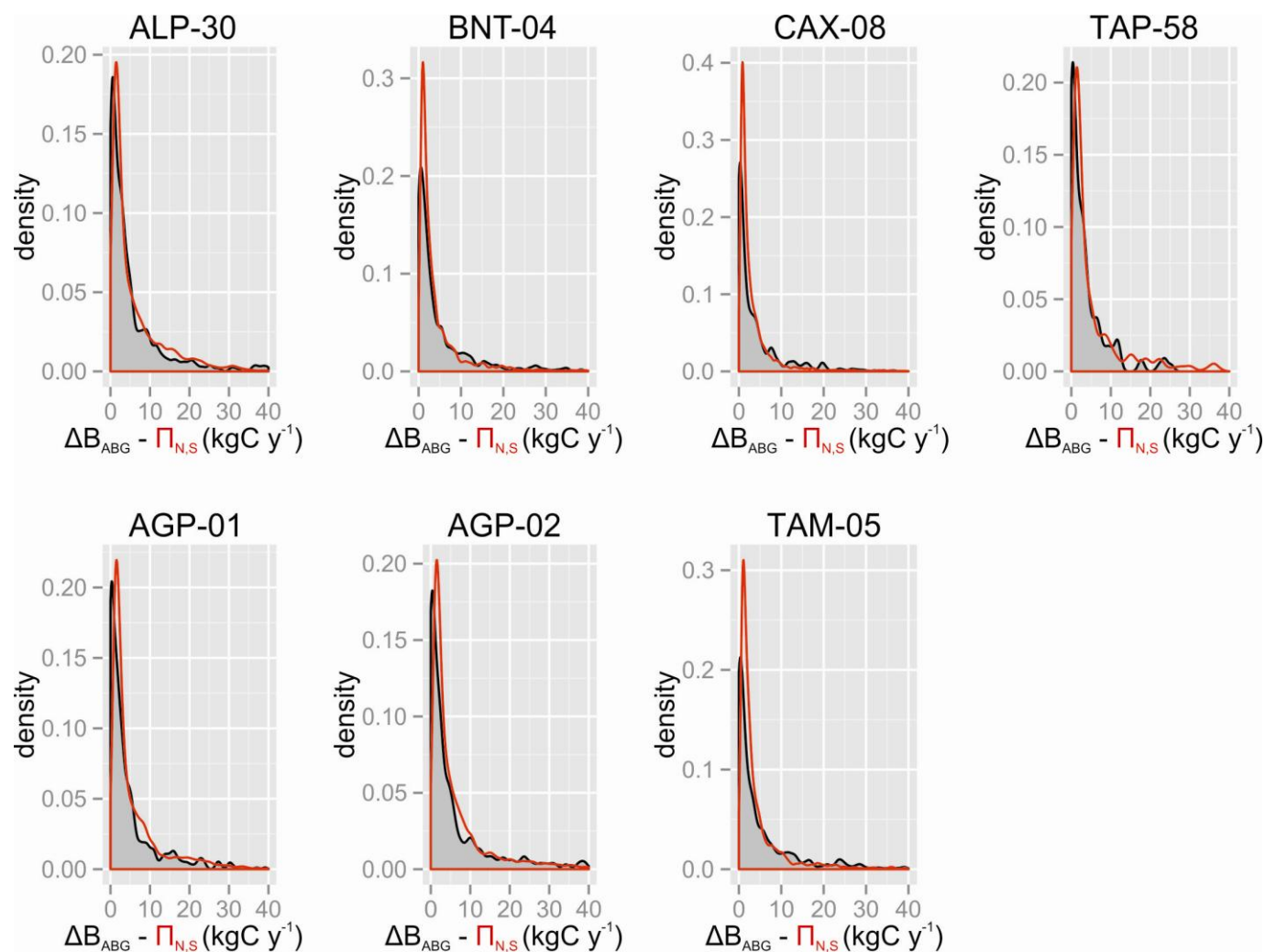
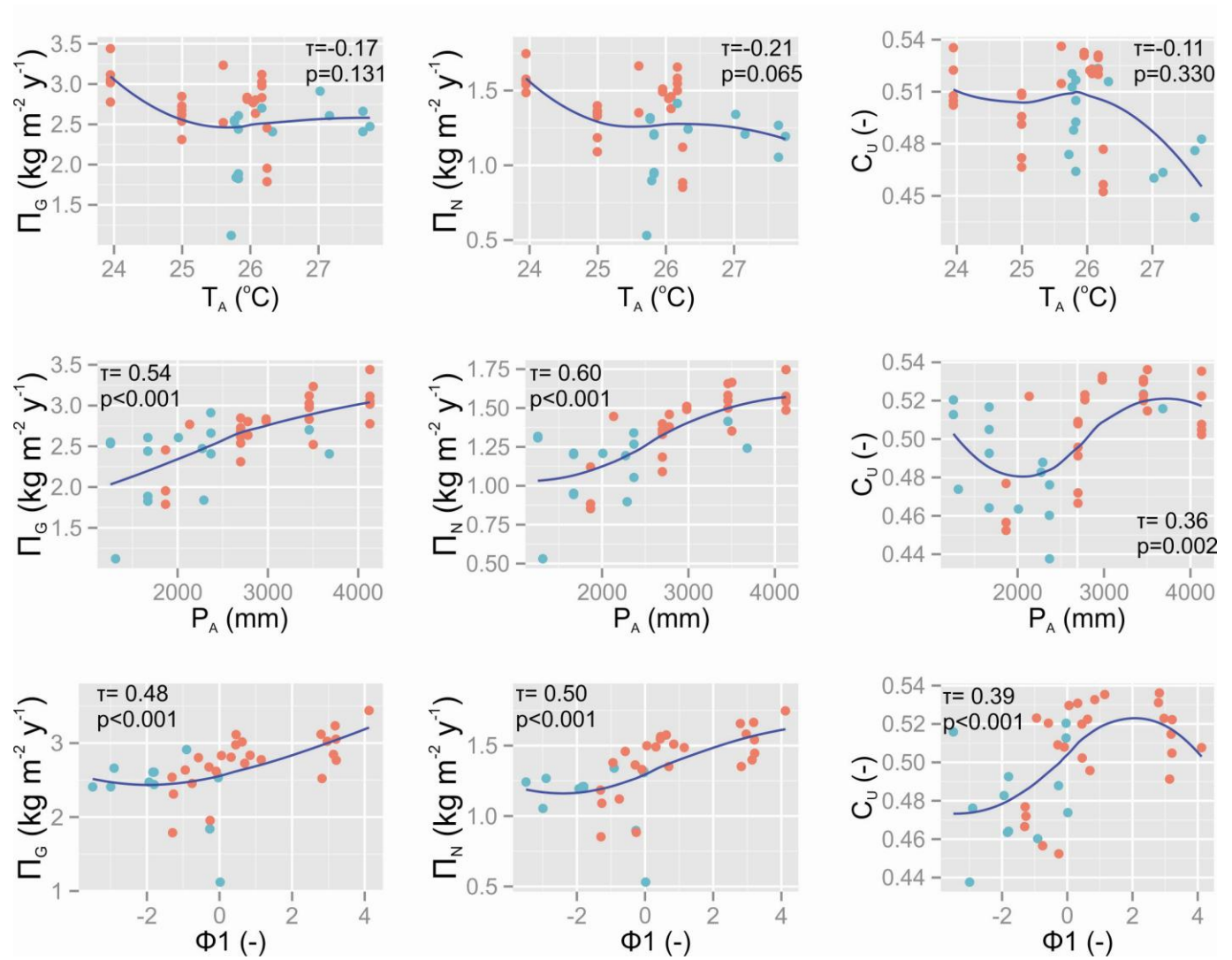


Figure S2.2: Simulated gross primary productivity (Π_G kgC m⁻² y⁻¹), net primary productivity (Π_N kgC m⁻² y⁻¹) and carbon use efficiency (C_U), along the annual temperature (T_A °C), annual precipitation (P_A mm) and fertility gradients (Φ_1) found across the 40 permanent measurement RAINFOR plots. Red dots indicate fertile plots while blue dots indicate infertile ones.



References

- Aragão, L., Malhi, Y., Metcalfe, D. B., Silva-Espejo, J. E., Jiménez, E., Navarrete, D., Almeida, S., Costa, A. C. L., Salinas, N. and Phillips, O. L.: Above-and below-ground net primary productivity across ten Amazonian forests on contrasting soils, *Biogeosciences*, 6(12), 2759–2778, 2009.
- Baker, T. R., Phillips, O. L., Laurance, W. F., Pitman, N. C. A., Almeida, S., Arroyo, L., DiFiore, A., Erwin, T., Higuchi, N. and Killeen, T. J.: Do species traits determine patterns of wood production in Amazonian forests?, *Biogeosciences*, 6(2), 297–307, 2009.
- Bernacchi, C. J., Singaas, E. L., Pimentel, C., Portis Jr, A. R. and Long, S. P.: Improved temperature response functions for models of Rubisco-limited photosynthesis, *Plant, Cell & Environment*, 24(2), 253–259, 2001.
- Brutsaert, W.: On a derivable formula for long-wave radiation from clear skies, *Water Resources Research*, 11(5), 742–744, 1975.
- Calvo-Alvarado, J. C., McDowell, N. G. and Waring, R. H.: Allometric relationships predicting foliar biomass and leaf area: sapwood area ratio from tree height in five Costa Rican rain forest species, *Tree physiology*, 28(11), 1601–1608, 2008.
- Cannell, M. G. R. and Thornley, J. H. M.: Modelling the components of plant respiration: some guiding principles, *Annals of Botany*, 85(1), 45–54, 2000.
- Chave, J., Andalo, C., Brown, S., Cairns, M. A., Chambers, J. Q., Eamus, D., Fölster, H., Fromard, F., Higuchi, N. and Kira, T.: Tree allometry and improved estimation of carbon stocks and balance in tropical forests, *Oecologia*, 145(1), 87–99, 2005.
- Domingues, T. F., Martinelli, L. A. and Ehleringer, J. R.: Seasonal patterns of leaf-level photosynthetic gas exchange in an eastern Amazonian rain forest, *Plant Ecology & Diversity*, (ahead-of-print), 1–15, 2013.
- Domingues, T. F., Meir, P., Feldpausch, T. R., Saiz, G., Veenendaal, E. M., Schrod, F., Bird, M., Djagbletey, G., Hien, F. and Compaore, H.: Co-limitation of photosynthetic capacity by nitrogen and phosphorus in West Africa woodlands, *Plant, Cell & Environment*, 33(6), 959–980, 2010.
- Enquist, B. J. and Niklas, K. J.: Global allocation rules for patterns of biomass partitioning in seed plants, *Science*, 295(5559), 1517–1520, 2002.
- Farquhar, G. D., von Caemmerer, S. von and Berry, J. A.: A biochemical model of photosynthetic CO₂ assimilation in leaves of C₃ species, *Planta*, 149(1), 78–90, 1980.
- Fyllas, N. M., Patino, S., Baker, T. de, Bielefeld Nardoto, G., Martinelli, L. A., Quesada, C. A., Paiva, R., Schwarz, M., Horna, V. and Mercado, L. M.: Basin-wide variations in foliar properties of Amazonian forest: phylogeny, soils and climate, *Biogeosciences*, 6(11), 2677–2708, 2009.
- Van Genuchten, M. T.: A closed-form equation for predicting the hydraulic conductivity of unsaturated soils, *Soil Science Society of America Journal*, 44(5), 892–898, 1980.
- Hodnett, M. G. and Tomasella, J.: Marked differences between van Genuchten soil water-retention parameters for temperate and tropical soils: a new water-retention pedo-transfer functions developed for tropical soils, *Geoderma*, 108(3), 155–180, 2002.
- Keenan, T., Sabate, S. and Gracia, C.: Soil water stress and coupled photosynthesis–conductance models: Bridging the gap between conflicting reports on the relative roles of stomatal, mesophyll conductance and biochemical limitations to photosynthesis, *Agricultural and Forest Meteorology*, 150(3), 443–453, 2010.

- Kerkhoff, A. J., Fagan, W. F., Elser, J. J. and Enquist, B. J.: Phylogenetic and growth form variation in the scaling of nitrogen and phosphorus in the seed plants, *The American Naturalist*, 168(4), E103–E122, 2006.
- Lloyd, J., Grace, J., Miranda, A. C., Meir, P., Wong, S. C., Miranda, H. S., Wright, I. R., Gash, J. H. C. and McIntyre, J.: A simple calibrated model of Amazon rainforest productivity based on leaf biochemical properties, *Plant, Cell & Environment*, 18(10), 1129–1145, 1995.
- Lloyd, J., Patino, S., Paiva, R. Q., Nardoto, G. B., Quesada, C. A., Santos, A. J. B., Baker, T. R., Brand, W. A., Hilke, I. and Gielmann, H.: Optimisation of photosynthetic carbon gain and within-canopy gradients of associated foliar traits for Amazon forest trees, *Biogeosciences*, 7(6), 1833–1859, 2010.
- Malhi, Y., Phillips, O. L., Lloyd, J., Baker, T., Wright, J., Almeida, S., Arroyo, L., Frederiksen, T., Grace, J., Higuchi, N., Killeen, T., Laurance, W. f., Leão, C., Lewis, S., Meir, P., Monteagudo, A., Neill, D., Núñez Vargas, P., Panfil, S. n., Patiño, S., Pitman, N., Quesada, C. a., Ruelas-Ll., A., Salomão, R., Saleska, S., Silva, N., Silveira, M., Sombroek, W. g., Valencia, R., Vásquez Martínez, R., Vieira, I. c. g. and Vinceti, B.: An international network to monitor the structure, composition and dynamics of Amazonian forests (RAINFOR), *Journal of Vegetation Science*, 13(3), 439–450, doi:10.1111/j.1654-1103.2002.tb02068.x, 2002.
- Medlyn, B. E., Duursma, R. A., Eamus, D., Ellsworth, D. S., Colin Prentice, I., Barton, C. V., Crous, K. Y., Angelis, P., Freeman, M. and Wingate, L.: Reconciling the optimal and empirical approaches to modelling stomatal conductance, *Global Change Biology*, 18(11), 3476–3476, 2012.
- Medlyn, B. E., Duursma, R. A., Eamus, D., Ellsworth, D. S., Prentice, I. C., Barton, C. V., Crous, K. Y., de Angelis, P., Freeman, M. and Wingate, L.: Reconciling the optimal and empirical approaches to modelling stomatal conductance, *Global Change Biology*, 17(6), 2134–2144, 2011.
- Medlyn, B. E., Pepper, D. A., O’Grady, A. P. and Keith, H.: Linking leaf and tree water use with an individual-tree model, *Tree Physiology*, 27(12), 1687–1699, 2007.
- Meinzer, F. C., Campanello, P. I., Domec, J.-C., Gatti, M. G., Goldstein, G., Villalobos-Vega, R. and Woodruff, D. R.: Constraints on physiological function associated with branch architecture and wood density in tropical forest trees, *Tree Physiology*, 28(11), 1609–1617, 2008.
- Meir, P., Grace, J. and Miranda, A. C.: Photographic method to measure the vertical distribution of leaf area density in forests, *Agricultural and Forest Meteorology*, 102(2), 105–111, 2000.
- Mori, S., Yamaji, K., Ishida, A., Prokushkin, S. G., Masyagina, O. V., Hagihara, A., Hoque, A. T. M. R., Suwa, R., Osawa, A., Nishizono, T., Ueda, T., Kinjo, M., Miyagi, T., Kajimoto, T., Koike, T., Matsuura, Y., Toma, T., Zyryanova, O. A., Abaimov, A. P., Awaya, Y., Araki, M. G., Kawasaki, T., Chiba, Y. and Umari, M.: Mixed-power scaling of whole-plant respiration from seedlings to giant trees, *PNAS*, 107(4), 1447–1451, doi:10.1073/pnas.0902554107, 2010.
- Niklas, K. J.: Modelling below-and above-ground biomass for non-woody and woody plants, *Annals of Botany*, 95(2), 315–321, 2005.
- Patiño, S., Fyllas, N. M., Baker, T. R., Paiva, R., Quesada, C. A., Santos, A. J. B., Schwarz, M., Steege, H. ter, Phillips, O. L. and Lloyd, J.: Coordination of physiological and structural traits in Amazon forest trees, *Biogeosciences*, 9(2), 775–801, 2012.
- Poorter, L., Bongers, L. and Bongers, F.: Architecture of 54 moist-forest tree species: traits, trade-offs, and functional groups, *Ecology*, 87(5), 1289–1301, 2006.

- Purves, D. W., Lichstein, J. W. and Pacala, S. W.: Crown plasticity and competition for canopy space: a new spatially implicit model parameterized for 250 North American tree species, *PLoS One*, 2(9), e870, 2007.
- Pury, D. de and Farquhar, G. D.: Simple scaling of photosynthesis from leaves to canopies without the errors of big-leaf models, *Plant, Cell & Environment*, 20(5), 537–557, 1997.
- Reich, P. B., Tjoelker, M. G., Pregitzer, K. S., Wright, I. J., Oleksyn, J. and Machado, J.-L.: Scaling of respiration to nitrogen in leaves, stems and roots of higher land plants, *Ecology Letters*, 11(8), 793–801, 2008.
- Ryan, M. G., Hubbard, R. M., Clark, D. A. and Sanford Jr, R. L.: Woody-tissue respiration for *Simarouba amara* and *Minquartia guianensis*, two tropical wet forest trees with different growth habits, *Oecologia*, 100(3), 213–220, 1994.
- Scheiter, S. and Higgins, S. I.: Impacts of climate change on the vegetation of Africa: an adaptive dynamic vegetation modelling approach, *Global Change Biology*, 15(9), 2224–2246, 2009.
- Taylor, M. S. and Thompson, J. R.: A data based algorithm for the generation of random vectors, *Computational Statistics & Data Analysis*, 4(2), 93–101, 1986.
- Tjoelker, M. G., Oleksyn, J. and Reich, P. B.: Modelling respiration of vegetation: evidence for a general temperature-dependent Q_{10} , *Global Change Biology*, 7(2), 223–230, 2001.
- Wang, Y.-P. and Leuning, R.: A two-leaf model for canopy conductance, photosynthesis and partitioning of available energy I: Model description and comparison with a multi-layered model, *Agricultural and Forest Meteorology*, 91(1), 89–111, 1998.